



Adsorption of ethyl violet dye in aqueous solution by forest wastes, wild carob

Abdelbaki Reffas^a, Abdallah Bouguettoucha^{b,*}, Derradji Chebli^b, Abdeltif Amrane^{c,d}

^aFaculté des sciences, Département de Chimie, Université Mohamed Bouafia, M'sila, Algeria, email: abdelbakireffas@gmail.com

^bLaboratoire de Génie des Procédés Chimiques (LGPC), Faculté de Technologie, Département de Génie des Procédés, Université Sétif-1, Elbez, 19000 Sétif, Algeria, Tel./Fax: +213 36 92 51 21; emails: abd_bouguettoucha@yahoo.fr (A. Bouguettoucha), derradji_chebli@yahoo.fr (D. Chebli)

^cEcole Nationale Supérieure de Chimie de Rennes, Université de Rennes 1, CNRS, UMR 6226, 11 allée de Beaulieu, CS 50837, 35708 Rennes Cedex 7, France, email: abdeltif.amrane@univ-rennes1.fr

^dUniversité européenne de Bretagne, Bd Laënnec, 35000 Rennes, France

Received 2 August 2014; Accepted 13 March 2015

ABSTRACT

The adsorption of basic dye (i.e. ethyl violet (EV) or basic violet 4) from aqueous solutions onto the forest waste non-modified wild carob (NMWC) was carried out by varying some process parameters, such as initial concentration, pH, and temperature. The experimental results showed that an increase in the pH from 2 to 7 led to a strong decrease in the adsorption capacity of the dye (EV) on NMWC, showing the predominance of the dispersion forces compared to the electrostatic interactions, owing to the cationic character of the dye and the pH_{pzc} of the biosorbent (~ 6). The adsorption process can be well described by means of a pseudo-second-order reaction model showing that boundary layer resistance was not the rate-limiting step, as confirmed by intraparticle diffusion. In addition, experimental data were accurately expressed by the Sips equation if compared with the Langmuir and Freundlich isotherms. The high “ m ” values of the Sips model characterized a multilayer adsorption and the maximum amount adsorbed given by the Sips model was 100.4 mg/g at 20°C, namely close to the experimental value and increased only weakly with the temperature. The values of ΔG^0 and ΔH^0 confirmed that the adsorption of EV on NMWC was spontaneous and endothermic in nature. The positive values of ΔS^0 suggested an irregular increase in the randomness at the NMWC–solution interface during the adsorption process.

Keywords: Adsorption; Wild carob; Isotherm models; Kinetics; Thermodynamic parameters

1. Introduction

Synthetic organic dyes have been widely used for dyeing of textile fibers such as cotton and polyester. However, these chemical materials often pose certain health hazards and environmental pollution. Dye

effluents, which are often discharged in aqueous effluents from the dyestuff manufacturing, dyeing and textile industries, may contain chemicals that exhibit toxic effects toward microbial populations and can be toxic and/or carcinogenic to mammalian animals [1]. Removal methods of dyes in industrial

*Corresponding author.

effluents may be traditionally divided into three main categories: physical, chemical, and biological processes [2,3]. Among them, physical adsorption is generally considered to be the most efficient method for quickly lowering the concentration of dissolved dyes in an effluent [1]. In this regard, activated carbon is the most widely used adsorbent for the removal of dyes from aqueous solutions. Despite the prolific use of this adsorbent throughout water/wastewater treatment and other industrial applications, the removal of organic pollutants by activated carbon adsorption remains an expensive process owing to the cost of both the adsorbent and its regeneration [4,5]. For these reasons, there is a growing interest in using low-cost alternatives as biosorbents [6–8]. Agricultural and forest waste materials such as baggage pith, saw dust, pine bark, maize cob, rice bran, rice hull, coconut husk fibers, nut shells, and cotton seed hulls have been evaluated as low-cost adsorbents for the removal of dyes and other toxic heavy metals [9–11]. However, their adsorption capacities (less than 40 mg/g-adsorbent) are far smaller than that of the activated carbon. Thus, great efforts are needed to exploit new promising adsorbents for the removal of dyes from aqueous solutions which therefore constitute important topics in the field of environmental technologies [12,13]. Non-modified wild carob (NMWC) was a waste itself and throughout the year, it can be found in abundant quantities in forest. To our knowledge, no work has been reported regarding its use for dye adsorption. This research may be therefore helpful to develop an alternative technology for its use. In the present study, powder of NMWC has been used as an adsorbent for the removal of ethyl violet (EV) from aqueous solutions. The purpose was to optimize the management of this important waste as a biosorbent. Therefore, the objectives of the present investigation were to investigate the interactions between EV and NMWC powder and to study the adsorption mechanism of EV onto this biosorbent.

2. Materials and methods

2.1. Preparation of the biosorbent

Wild carob (NMWC) used in this investigation was collected from forest (in Setif city, north east of Algeria). It was washed with distilled water to remove the surface-adhered particles and then dried at 80°C for 24 h to a constant weight, ground in a mortar to a very fine powder with diameter below or equal to 0.5 mm, and stored in a desiccator for further use.

2.2. Preparation of dye solution and determination of dye concentrations

EV (i.e. basic violet 4), a typical cationic dye (Fig. 1), was selected as a sorbate. EV dye is an Ethanaminium, N-(4-(bis (4-(diethylamino) phenyl) methylene)-2,5-cyclohexadien-1-ylidene)-N-éthyle-chloride, namely with the following formula, $C_{31}H_{42}ClN_3$. EV has a molecular weight of 492.158 g/mol and was obtained from ACROS with 90% purity. A stock solution of 50 mg/L was prepared by dissolving an appropriate amount (50 mg) of EV in a liter of distilled water. The working solutions were prepared by dilution of the stock solution with distilled water to yield the targeted concentrations. The pH of the solutions was adjusted by addition of either 0.1 M HCl or 0.1 M NaOH solutions. Before use, all bottles and glassware were beforehand cleaned and then rinsed with distilled water and oven dried at 60°C. An SP-8001 UV/VIS Spectrophotometer of Axiom (Germany, Shimadzu) was used to determine the residual dye concentrations in solution. After withdrawing samples at fixed time intervals and centrifugation, the supernatant was analyzed for residual EV at λ_{max} corresponding to the maximum adsorption for the dye solution ($\lambda_{max} = 596$ nm). Calibration curve was plotted between absorbance and concentration of the dye solution to obtain absorbance–concentration profile.

2.3. Analyses

2.3.1. Fourier transform infrared spectroscopy (FTIR) analysis

Infrared transmittance measurements of the wild carob (NMWC) were carried out on a Shimadzu 8400 SFTIR spectrometer at room temperature in the 400–4,000 cm^{-1} wavenumber range. Pellets made of a mixture of 1 mg of wild carob and 100 mg of KBr were pressed at high pressure and oven-dried 24 h at 110°C before analysis.

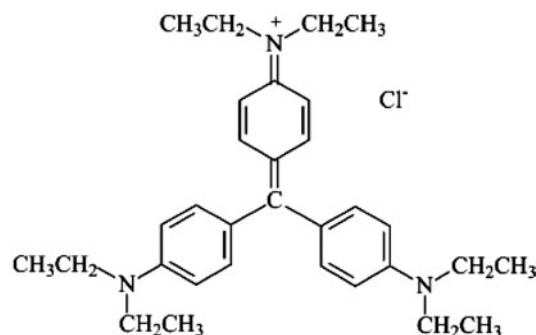


Fig. 1. Basic violet 4 chemical structure ($C_{31}H_{42}ClN_3$) (EV). MW: 492.14 $g\ mol^{-1}$.

2.3.2. Point of zero charge (pH_{pzc}) determination

The pH_{pzc} was determined by the so-called pH drift method. The pH of suspension of wild carob (NMWC) 50 mg and 50 ml of distilled water was adjusted to successive initial values between 2 and 12 with HCl (0,1 M) or NaOH (0,1 M). The suspensions were stirred 24 h and the final pH was measured and plotted versus the initial pH. The pH_{pzc} is determined at the value for which $pH_{final} = pH_{initial}$. The pH_{pzc} value of NMWC was found to be close to ~6 (Table 2).

2.3.3. Surface functional groups determination

In order to estimate the surface acidity or basicity, about 500 mg of sample (adsorbent NMWC) was mixed in a closed Erlenmeyer with 50 ml of 0.5 M aqueous reactant solution (NaOH or HCl). The suspension (mixture) was stirred for 24 h at a constant speed 200 rpm, at room temperature. Then the suspension was filtrated and the residual concentration of NaOH or HCl was achieved with HCl or NaOH (0.5 M) solution.

2.3.4. Scanning electron microscopy

Scanning electron microscopy (SEM) of treated NMWC before adsorption is visualized using Hitachi S-3000 N SEM at 7 kV and various magnifications, 100, 1,000, and 5,000.

3. Biosorption study

3.1. Kinetic experiments

Batch experiments of a given amount of adsorbent in 50 ml of dye solutions of a known concentration in a series of 250 mL conical flasks were carried out. Experiments were repeated five times.

The amount of dye adsorbed onto powder of NMWC at time t , Q_t (mg/g), was calculated by means of the following mass balance relationship:

$$Q_t = \frac{(C_0 - C_t)V}{m} \quad (1)$$

where C_0 is the initial dye concentration (mg/L), C_t is the concentration of dye at any time t , V is the volume of solution, and m is the mass of NMWC powder.

3.2. Equilibrium modeling

Equilibrium data, commonly known as adsorption isotherms, describe how adsorbates interact with

adsorbents and hence are critical in optimizing the use of adsorbents and provide information on the capacity of the adsorbent. To analyze interactions between powder of NMWC and EV, experimental data points were fitted to the Langmuir [14], Freundlich [15], and Sips [16] empirical models; they are the most frequently used two- and three-parameter equations in the literature describing non-linear equilibrium between adsorbed pollutant on the cells (Q_e) and pollutant in solution (C_e) at a constant temperature.

The Langmuir isotherm model assumes uniform energies of adsorption onto the adsorbent surface. Furthermore, the Langmuir equation is based on the assumption of the existence of monolayer coverage of the adsorbate at the outer surface of the adsorbent where all sorption sites are identical. The Langmuir equation [14] is given as follows:

$$\frac{Q_e}{Q_m} = \frac{K_L C_e}{1 + K_L C_e} \quad (2)$$

where Q_e is the equilibrium dye concentration on the adsorbent (mg/g); C_e , the equilibrium dye concentration in solution (mg/L); Q_m , the monolayer capacity of the adsorbent (mg/g); and K_L is the Langmuir constant.

A non-linear fit was performed by means of the Origin software in order to obtain the Langmuir model parameters. The parameter statistic “adjusted R -square” was also determined to identify the most accurate model to describe experimental results.

The Freundlich isotherm model assumes neither homogeneous site energies nor limited levels of sorption. The Freundlich model is the earliest known empirical equation and is shown to be consistent with exponential distribution of active centers, characteristic of heterogeneous surfaces [15]:

$$Q_e = K_F C_e^{1/n} \quad (3)$$

where Q_e is the equilibrium dye concentration on the adsorbent (mg/g); C_e , the equilibrium dye concentration in solution (mg/L); K_F and $1/n$ are empirical constants indicative of sorption capacity and sorption intensity, respectively. The Freundlich parameters were obtained by performing a non-linear fit (Origin software).

The Sips isotherm is a combination of the Langmuir and Freundlich isotherms [16]:

$$\frac{Q_e}{Q_m} = \frac{(k_s C_e)^m}{1 + (k_s C_e)^m} \quad (4)$$

where Q_m is the maximum monolayer biosorption (mg/g), k_s is the Sips constant solution (L/mg), and m the exponent of the Sips model.

4. Kinetic modeling

The study of adsorption dynamics described the solute adsorption rate. This rate controlled the residence time of adsorption at the solid–solution interface. Several kinetic models such as pseudo-first-order, pseudo-second-order, Elovich equation, and intraparticle diffusion models were applied to fit experimental data.

4.1. Pseudo-first-order equation

The pseudo-first-order kinetic model is the first equation for the adsorption of solid/liquid system based on the adsorption capacity. The linear form of the pseudo-first-order equation is given by Eq. (5) [17]:

$$\ln(Q_e - Q_t) = \ln Q_e - k_1 t \quad (5)$$

where Q_e (mg/g) and Q_t (mg/g) refer to the amount of dye adsorbed at equilibrium and at time t (min), respectively, and k_1 (1/min) is the equilibrium rate constant of pseudo-first-order equation. The rate constants are obtained from the straight line plots of $\ln(Q_e - Q_t)$ against t .

4.2. Pseudo-second-order equation

The pseudo-second-order model is based on the assumption of chemisorption of the adsorbate on the adsorbent [18]. This model is given by Eq. (6):

$$\frac{t}{Q_t} = \frac{1}{k_2 Q_e^2} + \frac{1}{Q_e} t \quad (6)$$

where k_2 (g/(mg min)) is the equilibrium rate constant of pseudo second-order equation. The straight line plot of t/Q_t versus t was considered to obtain the rate parameters.

4.3. The Elovich model

The linear form of Elovich equation is given by Eq. (7):

$$Q_t = \frac{1}{\beta} \ln(\alpha\beta) + \frac{1}{\beta} \ln t \quad (7)$$

where α is the initial adsorption rate constant (mg/(g min)) and the parameter β is related to the extent of surface coverage and activation energy for chemisorption (g/mg). The values of α and β can be calculated from the plot of Q_t against $\ln(t)$ [19,20].

4.4. Intraparticle diffusion model

Intraparticle diffusion model is commonly used to identify the adsorption mechanism for design purpose. According to Weber and Morris [21], for most adsorption processes, the uptake varies almost proportionately with $t^{1/2}$ rather than with the contact time and can be represented as follows:

$$Q_t = K_{id} t^{0.5} + C \quad (8)$$

where Q_t is the amount adsorbed at time t and $t^{0.5}$ is the square root of the time, C is the intercept and K_{id} (mg/g min^{0.5}) is the rate constant of intraparticle diffusion.

5. Results and discussion

5.1. Characterization

5.1.1. FTIR analysis

The infrared spectra were obtained (and transferred to Origin software) using Perkin–Elmer Spectrum One model FTIR spectrometer. The FTIR spectra before and after adsorption of NMWC are shown in Fig. 2. The functional groups before and after adsorption on NMWC and the corresponding infrared adsorption bands are shown in Table 1. EV were mainly caught by carboxylic (primarily present in pectin and hemicellulose but also extractives and lignin), phenolic (lignin and extractives) and to some extent hydroxylic (cellulose, hemicellulose, lignin, extractives, and pectin) and carbonyl groups (lignin) [22]. As shown in Fig. 2, the spectra displayed a number of adsorption peaks, indicating the active functional groups of NMWC. These peak shifts indicated that especially the bonded –OH groups, C–O stretching of ether groups, and C=C group played a major role in EV adsorption on NMWC [22]; they corresponded to the bands around 1,090 and 1,635 cm⁻¹ split, the tripled band at 3,443 cm⁻¹. The new band of low intensity which appeared at 3,250 cm⁻¹ after EV adsorption and which could be attributed to a ν (EV-biosorbent) constituted the most striking result.

The FTIR spectra of the NMWC (red line) show also absorption bands at 2,920 and 2,860 cm⁻¹ arising

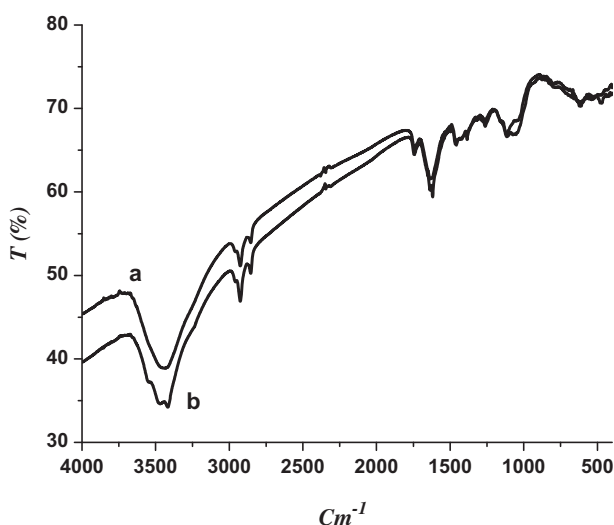


Fig. 2. FTIR spectra of NMWC before adsorption (a) and after adsorption (b).

from aliphatic C–H stretching in an aromatic methoxyl group, in methyl and methylene groups of side chains. The bands at 852 and 708 cm^{-1} are due to out-of-plane deformation mode of C–H for different substituted benzene rings. (This is confirmed by a strong band at 1,635 cm^{-1} due to C=C vibrations in aromatic rings.) The small band at about 1,720 cm^{-1} is usually assigned to C=O stretching vibrations of ketones, aldehydes, lactones, or carboxyl groups. The band at 1,450 cm^{-1} observed on the spectrum of NMWC can be assigned to the O–H bending band. The band at 1,257 cm^{-1} has been assigned to C–O stretching in acids, alcohols, phenols, ethers, and esters. The band

at 500 cm^{-1} is also observed for NMWC. This latter band can be attributed to –C–C– groups.

Fig. 2 shows also the FTIR spectra of EV after sorption (black line). The spectra indicate that lignin plays a significant role on EV sorption onto sorbent. This is confirmed by the shift of two characteristic bands associated to the lignin structure: the band associated to the aromatic ring vibrations (i.e. C=C bonds) and the band associated to the C–O stretching of the ether group (C–O–C) of the aromatic ring. The decrease in wavenumber of aromatic C=C band from 1,635 to 1,626 cm^{-1} could reflect π – π interactions between π aromatic rings donors of EV and π acceptor groups in the sorbent (i.e. aromatic rings of lignin) [23]. Concerning the bands attributed to C–O stretching (corresponding to the ether group of lignin), a shift in the band from 1,090 to 1,080 cm^{-1} for NMWC was observed. Nevertheless, it must be remarked that these bands can be also attributed to C–O bonds of cellulose/hemicelluloses constituents [23]. The band associated to the C–H bonds shifted from 2,920 to 2,939 cm^{-1} . This shift could reflect H– π interactions between aromatic rings from EV and methyl groups from lignin (–OCH₃) [23].

5.1.2. Surface functional groups determination

The NMWC was rather acid in agreement with its low content of basicity compared to its acidity. Table 2 shows less alkaline than acid groups confirming its acidic character. Thus, the lightly acid pH_{pzc} of NMWC can be attributed to the presence of oxygenated surface groups with a high pKa value.

Table 1

The FTIR spectral characteristics of NMWC before and after EV adsorption

IR peak	Adsorption bands (cm^{-1})			Assignment
	Before	After	Difference	
1	3,443	3,425	–18	Bonded –OH groups $\nu(\text{O–H})$
2	2,920	2,939	+19	C–H stretching $\nu(\text{C–H})$
3	2,854	2,854	0	C–H stretching $\nu(\text{C–H})$
4	1,720	1,720	0	C=O stretching $\nu(\text{C=O})$
5	1,635	1,626	–9	C=C vibrations $\nu(\text{C=C})$
6	1,500	1,490	–10	Secondary amine group $\nu(\text{N–H})$
7	1,450	1,423	–27	Carboxyl groups $\delta(\text{O–H})$
8	1,257	1,257	0	C–O valence vibration $\nu_{\text{as}}(\text{C–O–C})$ Carboxyl groups
9	1,090	1,080	–10	C–O stretching of ether groups $\nu_{\text{as}}(\text{C–O–C})$
10	852	825	0	C–H vibration $\gamma(\text{C–H})$
11	708	708	0	C–H vibration $\gamma(\text{C–H})$
12	500	444	–56	–C–C– groups

Note: ν : stretching; δ : bending (in-plane); γ : bending (out-of-plane); as: asymmetric.

Table 2
Surface characteristics of NMWC

Adsorbent	Acidity (meq g ⁻¹)	Basicity (meq g ⁻¹)	pH _{pzc} ~ 6
NMWC	4.22	4.05	~6

5.2. Influence of the pH

To study the influence of the pH on the adsorption capacity of the biosorbent NMWC for the cationic dye, EV, experiments were performed at an initial concentration of 50 mg/L and pH values ranging from 2 to 11 (Fig. 3). The cationic character of EV is due to the presence of the amine groups (Fig. 1), showing a pKa value of 1.3, and hence at pH range 2–11, amine groups are cationic. Adsorption can also be explained on the basis of an electrostatic interaction between the ionic dye molecule and the charged biosorbent substrate. The pH is known to affect the structural stability of dyes and therefore its color intensity [24]. At the considered pH range, 2–11, the biosorbent NMWC was negatively charged if the pH was superior to the pH_{pzc} ~ 6, while the biosorbent was positively charged for pH < pH_{pzc}. Since the highest adsorption uptake was measured at acidic pH 2, electrostatic interactions between the biosorbent and the EV cation at pH 6–11 did not favor adsorption. Thus, EV adsorption cannot be only controlled by electrostatic interactions.

Two possible mechanisms may be considered for EV removal [25–27]. One is the electrostatic interactions between the negative adsorption sites of the biosorbent (–COO⁻) and the positively charged dye. The other one is hydrogen bonding interactions between the reactive –OH on the biosorbent NMWC surface or –COOH groups of the biosorbent NMWC and the amine groups –N(C₂H₅)₂ of the dye. The biosorbent is slightly acidic, and has many carboxyl and hydroxyl groups which can increase interactions between the cationic groups of the dye and the carboxylic groups of the adsorbent. Hydrogen bonding may occur between hydroxyl or carboxyl groups on the surface of the biosorbent and amine groups on the dye molecules (Fig. 4). However, at alkaline pH (pH > 10), the screening effect of the counter ion, i.e. Na⁺ shields the charge of the ionized carboxyl groups on the biosorbent. As a result, the dye molecule is more difficult to transfer and the adsorbed amount of dye decreases. Additionally at pH < 6, the sorbent surface has more positive charges than negative ones. Thus, at very acidic conditions, carboxylic groups are probably protonated and the interaction that could

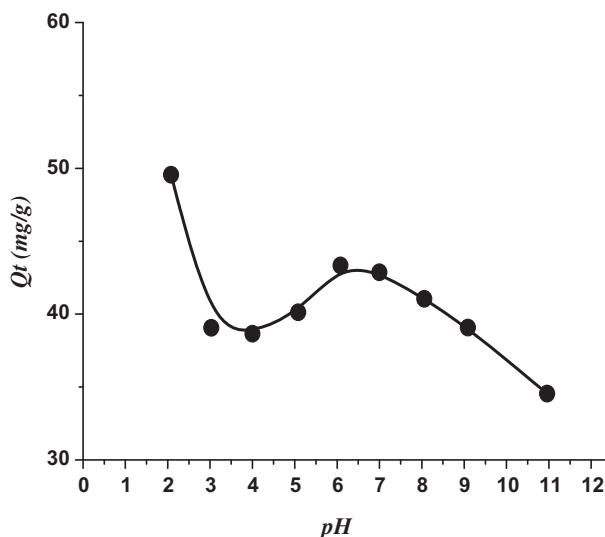


Fig. 3. Effect of pH on EV adsorption by NMWC.

occur between sorbent surface and the cationic dye (EV) could be favored by the *H*– π interactions between the π aromatic system of EV and –OH and –COOH groups [23].

5.3. Effect of the temperature

Experiments were carried out at three different temperatures (20, 40, and 60°C) and the results showed only a weak increase in the dye removal, from 43 to 45 mg/g, for temperatures increasing from 20 to 60°C (Fig. 5). From this, the impact of the temperature appeared not really significant.

5.4. Effect of the contact time and the initial dye concentration

The initial concentration provides an important driving force to overcome all mass transfer limitations between aqueous and solid phases, and hence dye removal is highly concentration dependent. To establish the equilibrium time for maximum uptake and to investigate the kinetics of the sorption process, the sorption of EV by NMWC was carried out for contact time ranging from 0 to 280 min (Fig. 6), showing a rapid dye sorption during the first minutes of experiments, before reaching a plateau at the end of the process. An increase in the initial dye concentration led to an increase in the sorption capacity, and irrespective of the initial dye concentration, equilibrium was achieved within few hours of adsorption.

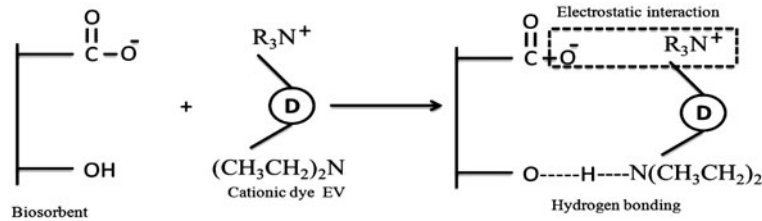


Fig. 4. Possible interaction mechanisms between the dye molecules and the biosorbent (NMWC).

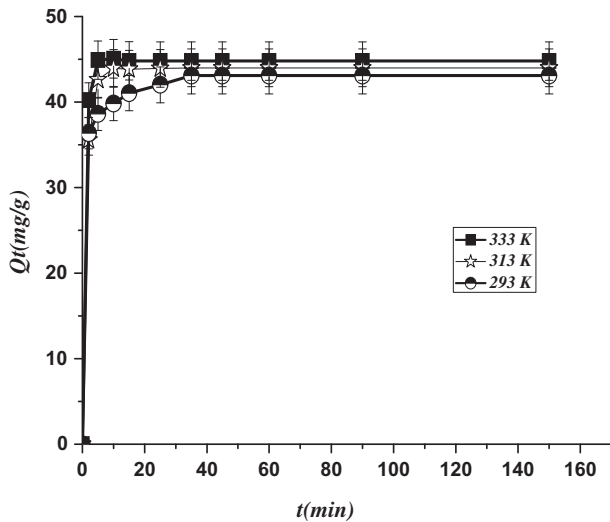


Fig. 5. Effect of temperature of EV adsorption by NMWC (pH 2).

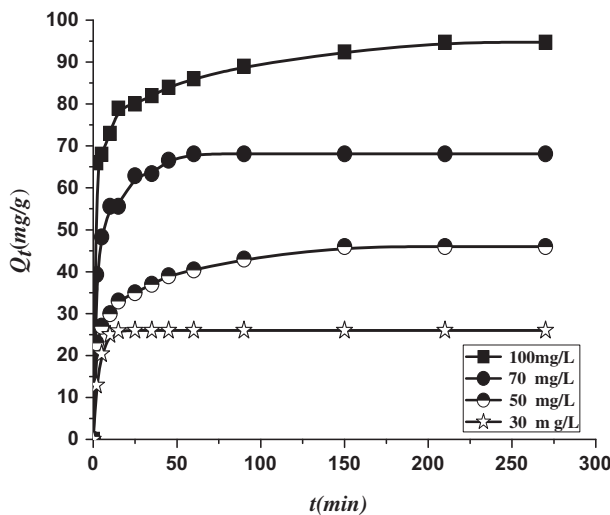


Fig. 6. Effect of the contact time on the biosorption capacity of EV onto NMWC at various concentrations ($T = 22 \pm 2^\circ\text{C}$, pH 2).

5.5. Biosorption kinetics

In order to investigate the adsorption mechanism, pseudo-first-order, pseudo-second-order, Elovich, and intraparticle kinetic equations were used to fit experimental data. The first-order kinetic equation was obviously not relevant, since no straight lines were obtained (results not shown). It was in agreement with other findings, showing that the first-order equation of Lagergren [17] does not always fit accurately the whole process; it is generally applicable over the initial stage of the adsorption process. The Elovich model also appeared inappropriate; while only the pseudo-second-order model led to high regression coefficients for all tested dye concentrations (Table 3) and the corresponding fittings are displayed in Fig. 7. According to Canzano et al. [28], the data at or near the equilibrium have been omitted because higher t values led to extremely high errors. The Q_e values estimated from the pseudo-second-order kinetic model were also in agreement with experimental data (Table 3) for all tested dye concentrations (Fig. 7), and the results suggested that boundary layer resistance was not the rate-limiting step since dye biosorption followed pseudo-second-order kinetics [29].

The effect of intraparticle diffusion resistance on adsorption was evaluated by intraparticle diffusion model to identify the adsorption mechanism [30] as expressed in Eq. (9). A plot of Q_t against $t^{0.5}$ should give a linear line whose slope is K_{id} (Fig. 8); the values of K_{id} are listed in Table 3. The plot of Q_t versus $t^{0.5}$ was linear within a certain extent but not linear over the whole time range. It can be separated into two or more linear regions. The first straight portion could be attributed to macropore diffusion (step 1), namely the transport of dye molecules from the bulk solution to the surface of the adsorbent; while the second linear portion could be attributed to micropore diffusion (step 2), namely the binding of the dye molecules on the active sites of biosorption. Since the linear plots did not pass through the origin, it is clear that intraparticle diffusion was not the only rate-limiting mechanism for the biosorption of EV onto NMWC from aqueous solutions [31–33].

Table 3
Parameters of kinetic models for adsorption of EV onto NMWC ($T = 22 \pm 2^\circ\text{C}$, pH 2)

C (mg/L)	Pseudo-first-order			Pseudo-second-order			Elovich Model			Intraparticle diffusion model			
	Q_{exp} (mg/g)	Q_e (mg/g)	K_1 (min^{-1})	R^2	Q_{exp} (mg/g)	Q_e (mg/g)	$K_2 \cdot 10^5$ (g/mg min)	R^2	α (mg/g min)	β (g/mg)	R^2	K_{id} (mg/g $\text{min}^{0.5}$)	R^2
30	25.75	30.49	0.019	0.80	25.75	26.00	3.25	0.9999	295	0.085	0.60	6.91	0.95
50	46.08	36.28	0.069	0.90	46.08	48.00	8.97	0.9990	140.42	0.106	0.87	2.41	0.96
70	68.07	24.01	0.025	0.88	68.07	68.77	0.047	0.9998	40.10	0.147	0.72	4.75	0.92
100	95.01	29.45	0.360	0.91	95.01	97.75	1.54	0.9999	80.36	0.280	0.66	3.23	0.94

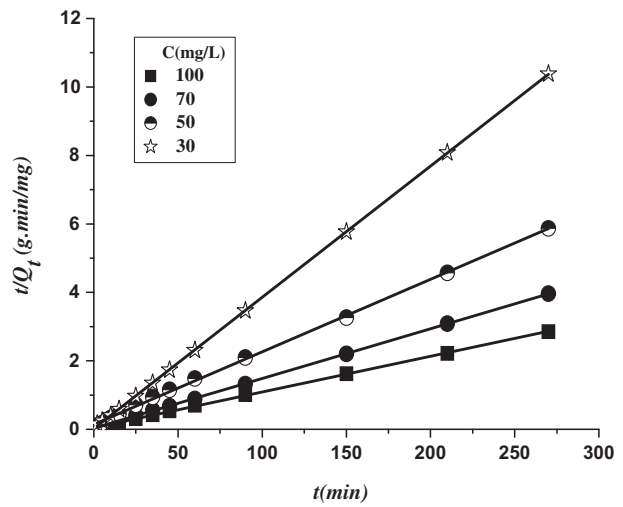


Fig. 7. Pseudo-second-order kinetic plots for adsorption of EV on NMWC at various concentrations ($T = 22 \pm 2^\circ\text{C}$, pH 2).

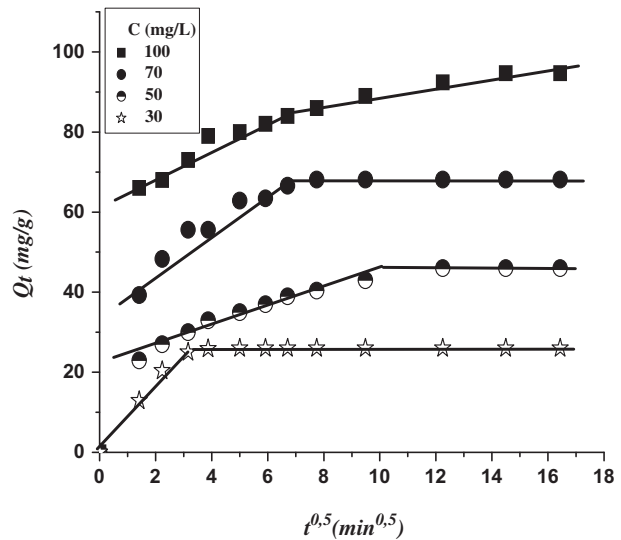


Fig. 8. Intraparticle diffusion kinetic plots for adsorption of EV on NMWC at various concentrations ($T = 22 \pm 2^\circ\text{C}$, pH 2).

5.6. Isotherm analysis

Adsorption isotherms of EV onto NMWC at two pH values are displayed in Fig. 9, showing that the pH of the medium affects significantly the adsorbed amounts, which were higher for pH 2 if compared to pH 7; and adsorption uptake were 98 and 55 mg/g for pH 2 and 7, respectively. Adsorption can also be explained on the basis of an electrostatic interaction between the ionic dye molecule and the charged

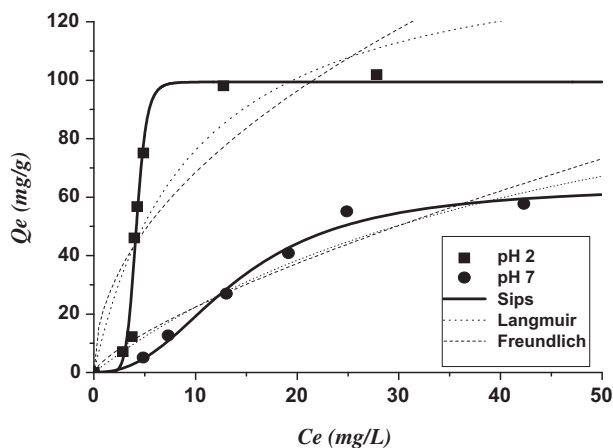


Fig. 9. Equilibrium isotherms for EV onto NMWC. Comparison between the experimental data (points) and predictions of the Langmuir, Freundlich, and Sips models (lines).

NMWC substrate. Indeed, according to the pH_{pzc} value, 6, the biosorbent is positively and negatively charged at pH 2 and 7, respectively. An increase in pH from 2 to 7 led to a strong decrease in the adsorption capacity of the dye (EV) on the NMWC sample. The adsorption of the cationic dyes is favored on acidic materials by mechanisms involving to some extent electrostatic forces, but the main role is played by the dispersive forces. These results can be therefore justified by a mechanism involving the predominance of the dispersion forces compared to the electrostatic interactions (Fig. 4).

For any given system, a correct mathematical description of equilibrium adsorption capacity is indispensable for reliable prediction of adsorption parameters and quantitative comparison of adsorption behavior for different adsorbent systems (or for varied experimental conditions). In order to optimize the design of an adsorption system, it is important to establish the most appropriate correlation for the equilibrium curve. Several equilibrium adsorption isotherm models are available, and the most common ones are

the monolayer adsorption developed by Langmuir [14], the multilayer adsorption of Freundlich [15], and the Sips isotherm [16]. Experimental data of EV on NMWC were fitted to the isotherm models using Origin software and the graphical representations of these models are presented in Fig. 9 and all constants are collected in Table 4. It can be seen in Fig. 9 that both model Langmuir and Freundlich did not describe accurately the adsorption behavior of EV from aqueous solution onto NMWC, as reflected by the correlation coefficients (R^2), 0.79 and 0.73, respectively (Table 4). Contrarily, the sips model described satisfactorily experimental data (Fig. 9) leading to correlation coefficients R^2 close to 1 (Table 4). The high “ m ” values of the Sips model (Eq. (5)—Table 4) confirmed that EV sorption onto NMWC occurred by the formation of a multilayer. The maximum biosorption capacity (Q_m) obtained from the Sips model was 100.4 mg/g for pH 2 at 293 K, namely close to the experimental value. It should be noted that the comparison with literature data was not easy, owing to the lack of related studies.

5.7. Thermodynamic analysis

The thermodynamic parameters reflect the feasibility and the spontaneous nature of a biosorption process. Parameters such as the free energy change (ΔG), the enthalpy change (ΔH), and the entropy change (ΔS) can be estimated using equilibrium constants varying with temperature. The free energy change of the adsorption reaction is given using Eq. (9) as reported by Milonjic [34] and Canzano et al. [35]:

$$\Delta G^0 = -RT \ln \rho(K_C) \quad (9)$$

where ΔG^0 is the free energy change (kJ mol^{-1}), R the universal gas constant ($8.314 \text{ J mol}^{-1} \text{ K}^{-1}$), T the absolute temperature (K), K_C the thermodynamic equilibrium constant (L g^{-1}) (Eq. (12)), and ρ the water density (g L^{-1}). ΔH^0 and ΔS^0 values of the biosorption process were calculated from the Van't Hoff Eq. (10):

Table 4
Isotherm constants and correlation coefficients for EV adsorbed on NMWC

pH	Langmuir			Freundlich			Sips			
	K_L (L/mg)	Q_e (mg/g)	R^2	K_f (mg/g)	n_F	R^2	Q_m (mg/g)	K_{LF} (L/mg)	m	R^2
2	0.104	149.13	0.79	22.02	2.03	0.73	99.40	0.24	8.82	0.98
7	0.02	134.3	0.94	4.12	1.36	0.92	64.02	0.07	2.37	0.99

Table 5

Thermodynamic parameters for adsorption of EV at various temperatures ($T = 22 \pm 2^\circ\text{C}$, pH 2)

Dye: Ethyl violet	T (K)	ΔG^0 (kJ mol $^{-1}$ K $^{-1}$)	ΔH^0 (kJ mol $^{-1}$ K $^{-1}$)	ΔS^0 (J mol $^{-1}$ K $^{-1}$)
	293	-21.28	6.47	94.72
	313	-23.17		
	333	-25.07		

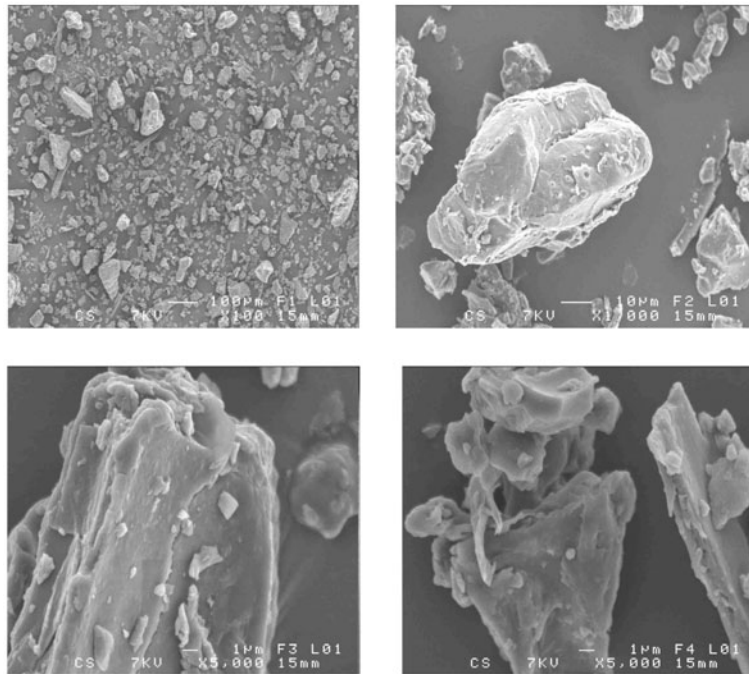


Fig. 10. SEM images of NMWC before adsorptions.

$$\ln(\rho K_C) = -\frac{\Delta H^0}{RT} + \frac{\Delta S^0}{R} \quad (10)$$

$$K_C = \frac{Q_e}{C_e} \quad (11)$$

ΔH and ΔS can be then deduced from the slope ($\Delta H/R$) and the intercept ($\Delta S/R$) of the plot of $\ln(\rho K_C)$ versus $1/T$. The calculated thermodynamic parameters are given in Table 5.

In general, the change in free energy for physisorption is between -20 and 0 kJ/mol and in a range of -80 to -400 kJ/mol for chemisorption [36]. The result obtained, about -20 kJ/mol for all tested temperatures, was characteristic of a spontaneous physisorption process; it was in agreement with the low impact of the temperature on EV adsorption (Fig. 5). The positive value of entropy change suggested an

increasing randomness at the solid–solution interface during the adsorption of EV on the biosorbent.

5.8. Scanning micrograph (SEM)

The SEM surface images of (NMWC) (Fig. 10) observed at a one micron meter scale were almost similar, showing a homogenous surface and a smooth surface morphology. By contrast, the $10 \mu\text{m}$ scale SEM image displays few microspores and a relatively heterogeneous surface morphology.

6. Conclusion

Wild carob (NMWC) was investigated for the removal of cationic dye (EV) from aqueous solution and the following conclusions can be drawn from the results of the present study:

- The adsorption capacity was found to be 98 mg/g at pH 2.
- Adsorption isotherm data were accurately described by the Sips isotherm, while kinetic data were accurately fitted by the pseudo-second-order kinetic model.
- The negative values of ΔG^0 revealed that the adsorption process was spontaneous. The positive values of ΔH^0 and ΔS^0 showed the endothermic nature and an increase in disorder of EV molecules during the sorption process, respectively.
- The pH of the medium influenced significantly the adsorbed amounts; an increase in pH from 2 to 7 led to a strong decrease in the adsorption capacity of the dye (EV) on the sample (NMWC).

References

- [1] J. Sokolowska-Gajda, H.S. Freeman, A. Reife, Chemical removal of phosphate ions from disperse dye filtrates, in: H.S. Freeman, A. Reife (Eds.), *Environmental Chemistry of Dyes and Pigments*, John Wiley & Sons, Inc., New York, NY, 1996, pp. 239–251.
- [2] Y.M. Slokar, A. Majcen-Le Marechal, Methods of decoloration of textile wastewaters, *Dyes Pig.* 37 (1998) 335–356.
- [3] O.J. Hao, H. Kim, P.C. Chiang, Decolorization of wastewater, *Crit. Rev. Environ. Sci. Technol.* 30 (2000) 449–505.
- [4] Y.C. Sharma, Optimization of parameters for adsorption of methylene blue on a low-cost activated carbon, *J. Chem. Eng. Data* 55 (2010) 435–439.
- [5] S. Wang, Z.H. Zhu, A. Coomes, F. Haghseresht, G.Q. Lu, The physical and surface chemical characteristics of activated carbons and the adsorption of methylene blue from wastewater, *J. Colloid Interface Sci.* 284 (2005) 440–446.
- [6] Z. Aksu, Application of biosorption for the removal of organic pollutants: A review, *Process Biochem.* 40 (2005) 997–1026.
- [7] Z. Aksu, S. Tezer, Biosorption of reactive dyes on the green alga *Chlorella vulgaris*, *Process Biochem.* 40 (2005) 1347–1361.
- [8] M.M. Abd El-Latif, A.M. Ibrahim, M.F. El-Kady, Adsorption equilibrium, kinetics and thermodynamics of methylene blue from aqueous solutions using biopolymer oak sawdust composite, *J. Am. Sci.* 6 (2010) 267–283.
- [9] A. Sultana, Equilibrium and kinetic evaluation of the adsorption of commercial brilliant red on used black tea leaves, MS Thesis, University of Dhaka, Bangladesh, 2006.
- [10] S. Bailey, T.J. Olin, R.M. Bricka, D. Adrian, A review of potentially low-cost sorbents for heavy metals, *Wat. Res.* 33 (1999) 2469–2479.
- [11] D. Chebli, A. Bouguettoucha, T. Mekhalif, S. Nacef, A. Amrane, Valorization of an agricultural waste, *Stipa tonacissima* fibers, by biosorption of an anionic azo-dye, Congo red, *Desalin. Water Treat.* 54 (2015) 245–254, doi: 10.1080/19443994.2014.880154.
- [12] S. Dawood, T.K. Sen, Removal of anionic dye Congo red from aqueous solution by raw pine and acid-treated pine cone powder as adsorbent Equilibrium, thermodynamic, kinetics, mechanism and process design, *Water Res.* 46 (2012) 1933–1946.
- [13] F. Deniz, S.D. Saygideger, Equilibrium, kinetic and thermodynamic studies of Acid Orange 52 dye biosorption by *Paulownia tomentosa* Steud. Leaf powder as a low-cost natural biosorbent, *Bioresour. Technol.* 101 (2010) 5137–5143.
- [14] I. Langmuir, The adsorption of gases on plane surfaces of glass, mica and platinum, *J. Am. Chem. Soc.* 40 (1918) 1361–1403.
- [15] H.M.F. Freundlich, Ober dies adsorption in Losungen (About adsorption in solution), *Z. Phys. Chem.* 57 (1906) 385–470.
- [16] G.L. Dotto, M.L.G. Vieira, V.M. Esquerdo, L.A.A. Pinto, Equilibrium and thermodynamics of azo dyes biosorption onto *Spirulina platensis*, *Braz. J. Chem. Eng.* 30 (2013) 13–21.
- [17] S. Lagergren, Zur Theorie der sogenannten Adsorption gelöster Stoffe (On the theory of so-called adsorption of solutes), *K. Sven. Vetenskapskad. Handl.* 24 (1898) 1–39.
- [18] V.C. Srivastava, I.D. Mall, I.M. Mishra, Adsorption of toxic metal ions onto activated carbon, *Chem. Eng. Process.* 47 (2008) 1269–1280.
- [19] H. Yan, W. Zhang, X. Kan, L. Dong, Z. Jiang, H. Li, H. Yang, R. Cheng, Sorption of methylene blue by carboxymethyl cellulose and reuse process in a secondary sorption, *Colloids Surf. A* 380 (2011) 143–151.
- [20] Y. Önal, Kinetics of adsorption of dyes from aqueous solution using activated carbon prepared from waste apricot, *J. Hazard. Mater.* 137 (2006) 1719–1728.
- [21] W.J. Weber, J.C. Morris, Equilibrium and capacities for adsorption on carbon, *J. Sanit. Eng. Div. ASCE* 89 (1963) 31–60.
- [22] E. Malkoc, Y. Nuhoglu, Y. Abali, Cr(VI) adsorption by waste acorn of *Quercus ithaburensis* in fixed beds: Prediction of breakthrough curves, *Chem. Eng. J.* 119 (1) (2006) 61–68.
- [23] M.A. Olivella, N. Fiol, F. de la Torre, J. Poch, I. Villaescusa, Assessment of vegetable wastes for basic violet 14 removal: Role of sorbent surface chemistry and porosity, *Desalin. Water Treat.* (2013) 1–11.
- [24] I.D. Mall, V.C. Srivastava, N.K. Agarwal, I.M. Mishra, Removal of congo red from aqueous solution by bagasse fly ash and activated carbon: Kinetic study and equilibrium isotherm analyses, *Chemosphere* 61 (4) (2005) 492–501.
- [25] E. Karadağ, Ö.B. Üzümlü, D. Saraydin, Swelling equilibria and dye adsorption studies of chemically cross-linked superabsorbent acrylamide/maleic acid hydrogels, *Eur. Polym. J.* 38 (2002) 2133–2141.
- [26] G.R. Mahdavinia, A. Pourjavadi, H. Hosseinzadeh, M.J. Zohuriaan, Modified chitosan 4. Superabsorbent hydrogels from poly(acrylic acid-co-acrylamide) grafted chitosan with salt- and pH-responsiveness properties, *Eur. Polym. J.* 40 (2004) 1399–1407.
- [27] D. Şolpan, Z. Kölge, Adsorption of methyl violet in aqueous solutions by poly(N-vinylpyrrolidone-co-methacrylic acid) hydrogels, *Radiat. Phys. Chem.* 75 (2006) 120–128.

- [28] S. Canzano, P. Iovino, V. Leone, S. Salvestrini, S. Capasso, Use and misuse of sorption kinetic data: A common mistake that should be avoided, *Adsorpt. Sci. Technol.* 30 (2012) 217–226.
- [29] X.J. Xiong, X.J. Meng, T.L. Zheng, Biosorption of C.I. Direct Blue 199 from aqueous solution by nonviable *Aspergillus niger*, *J. Hazard. Mater.* 175 (2010) 241–246.
- [30] M.S. Chiou, H.Y. Li, Adsorption behavior of reactive dye in aqueous solution on chemical cross-linked chitosan beads, *Chemosphere* 50 (2003) 1095–1105.
- [31] K. Porkodi, K. Vasanth Kumar, Equilibrium, kinetics and mechanism modeling and simulation of basic and acid dyes sorption onto jute fiber carbon: Eosin yellow, malachite green and crystal violet single component systems, *J. Hazard. Mater.* 143(1–2) (2007) 311–327.
- [32] A. Mittal, Adsorption kinetics of removal of a toxic dye, Malachite Green, from wastewater by using hen feathers, *J. Hazard. Mater.* 133(1–3) (2006) 196–202.
- [33] Z. Baysal, E. Çinar, Y. Bulut, H. Alkan, M. Dogru, Equilibrium and thermodynamic studies on biosorption of Pb(II) onto *Candida albicans* biomass, *J. Hazard. Mater.* 161(1) (2009) 62–67.
- [34] S.K. Milonjic, A consideration of the correct calculation of thermodynamic parameters of adsorption, *J. Serb. Chem. Soc.* 72 (2007) 1363–1367.
- [35] S. Canzano, P. Iovino, S. Salvestrini, S. Capasso, Comment on Removal of anionic dye Congo red from aqueous solution by raw pine and acid-treated pine cone powder as adsorbent: Equilibrium, thermodynamic, kinetics, mechanism and process design, *Water Res.* 46 (2012) 4314–4315.
- [36] D. Myers, *Surfaces, Interfaces, and Colloids: Principles and Applications*, second ed., Wiley, New York, NY, 1999, pp. 187–190.